

## Junction and carrier temperature measurements in deep-ultraviolet light-emitting diodes using three different methods

Y. Xi, J.-Q. Xi, Th. Gessmann, J. M. Shah, J. K. Kim, and E. F. Schubert<sup>a)</sup>

*Future Chips Constellation, Department of Electrical, Computer, and Systems Engineering and Department of Physics, Applied Physics, and Astronomy, Rensselaer Polytechnic Institute, Troy, New York 12180*

A. J. Fischer, M. H. Crawford, K. H. A. Bogart, and A. A. Allerman

*Compound Semiconductor Research Laboratory, Sandia National Laboratories, Albuquerque, New Mexico 87185*

(Received 13 August 2004; accepted 9 November 2004; published online 11 January 2005)

The junction temperature of AlGaIn ultraviolet light-emitting diodes emitting at 295 nm is measured by using the temperature coefficients of the diode forward voltage and emission peak energy. The high-energy slope of the spectrum is explored to measure the carrier temperature. A linear relation between junction temperature and current is found. Analysis of the experimental methods reveals that the diode-forward voltage is the most accurate ( $\pm 3$  °C). A theoretical model for the dependence of the diode forward voltage ( $V_f$ ) on junction temperature ( $T_j$ ) is developed that takes into account the temperature dependence of the energy gap. A thermal resistance of 87.6 K/W is obtained with the device mounted with thermal paste on a heat sink. © 2005 American Institute of Physics. [DOI: 10.1063/1.1849838]

III-V nitride semiconductors have a direct band gap and thus are very suitable solid-state ultraviolet (UV) light sources. Such UV sources have a wide variety of applications, including UV-induced fluorescence, spectrofluometry, sanitation, communications, photo-catalytic processes, high resolution optics, lighting, and displays. Double heterostructure GaInN/AlGaIn UV light-emitting diodes (LEDs) emitting at 371 nm with external quantum efficiency of 7.5% and output powers of 5 mW have been demonstrated.<sup>1</sup> In the deep UV, devices emitting 1.3 mW at 290 nm were recently demonstrated by Sandia National Laboratories.<sup>2</sup> Recent improvements in high-power UV emitters include epitaxial lift-off<sup>3</sup> and a micro-pixel design to reduce parasitic resistances.<sup>4,5</sup> The junction temperature is a critical parameter and affects internal efficiency, maximum output power, and reliability. Several groups have reported measurements of the junction temperature of laser diodes using micro-Raman spectroscopy,<sup>6</sup> thermal resistance,<sup>7</sup> photothermal reflectance microscopy,<sup>8</sup> electroluminescence,<sup>9</sup> and photoluminescence.<sup>10</sup> A noncontact method based on the emission peak ratio has been demonstrated for a white dichromatic LED source.<sup>11</sup>

In this letter, three methods are employed to measure the junction and carrier temperature of AlGaIn UV LEDs emitting at 295 nm.

From the well-known Shockley equation,<sup>ERROR</sup> for a forward voltage  $V_f \gg kT/e$ , we obtain

$$\frac{dV_f}{dT} = \frac{d}{dT} \left[ \frac{n_{\text{ideal}} kT}{e} \ln \left( \frac{J_f}{J_s} \right) \right], \quad (1)$$

where  $J_s$  is the saturation current density,  $n_{\text{ideal}}$  is the diode ideality factor, and the other symbols have their usual meaning.<sup>12</sup> The saturation current density depends on the diffusion constants of electrons and holes, the lifetimes of electrons and holes, the effective density of states at the conduc-

tion band and valence band edge, and the band gap energy, all of which depend on the junction temperature. Substituting the temperature dependencies of these quantities (using  $\mu \propto T^{-3/2}$  for phonon scattering,  $D \propto T^{-1/2}$ , and  $N_C$  and  $N_V \propto T^{3/2}$ ) into Eq. (1) and executing the derivative yields

$$\frac{dV_f}{dT} = \frac{eV_f - E_g}{eT} + \frac{1}{e} \frac{dE_g}{dT} - \frac{3k}{e}. \quad (2)$$

This equation gives the fundamental temperature dependence of the forward voltage and includes the temperature dependence of the energy gap which in prior work had been neglected.<sup>13</sup> The first, second, and third summand on the right-hand side of the equation is due to the temperature dependence of the intrinsic carrier concentration, band gap energy, and the effective densities of states  $N_C$  and  $N_V$ , respectively. LEDs are typically operated at forward voltages close to the built-in voltage, i.e.,  $V_f \approx V_{\text{bi}}$ . For nondegenerate doping concentrations, we can thus write

$$eV_f - E_g \approx kT \ln \left( \frac{N_D N_A}{N_C N_V} \right). \quad (3)$$

Furthermore, the band gap energy can be expressed as  $E_g = E_0 - \alpha T^2 / (\beta + T)$  where  $\alpha$  and  $\beta$  are the Varshni parameters. Substituting Eq. (3) into Eq. (2) and using the Varshni parameters yields

$$\frac{dV_f}{dT} \approx \frac{k}{e} \ln \left( \frac{N_D N_A}{N_C N_V} \right) - \frac{\alpha T (T + 2\beta)}{e(T + \beta)^2} - \frac{3k}{e}. \quad (4)$$

This equation is a very useful expression for the temperature coefficient of the forward voltage. For GaN diodes, the calculated  $dV_f/dT = -1.76$  mV/K is in good agreement with the experimental value of  $-2.3$  mV/K.<sup>12</sup>

The diode forward voltage is used to assess the temperature of a  $p$ - $n$  junction by first conducting a calibration measurement and subsequently the junction-temperature measurement. In the calibration, a pulsed forward current drives the LED which is located in the temperature-controlled

<sup>a)</sup>Electronic mail: efschubert@rpi.edu

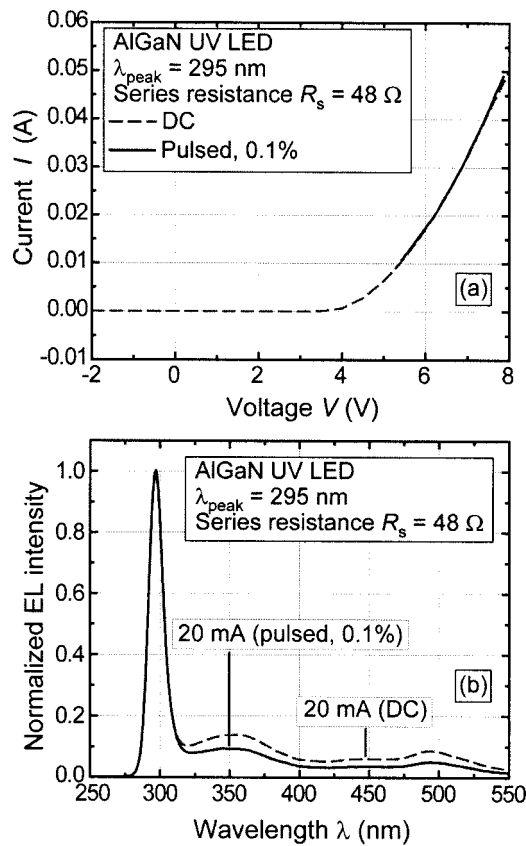


FIG. 1. (a) Current–voltage curve and (b) emission spectra under pulsed and dc condition for AlGaIn deep UV LED.

ambient of an oven. A small duty cycle of 0.1% ensures that the junction temperature is equal to the ambient temperature. The pulsed forward voltage and current of the device are measured with an oscilloscope at different ambient temperatures. The calibration measurement thus establishes the relation between  $V_f$  and  $T_j$ .

In the same calibration measurement, the emission peak energy is recorded which allows one to deduce the junction temperature from the shift of the peak energy with temperature. The high-energy slope of emission spectrum for a non-degenerate semiconductor follows the proportionality  $I \propto \exp(-E/kT)$ .<sup>14</sup> Thus, the high-energy slope allows one to deduce the carrier temperature as a function of current.

To demonstrate the viability of the methods, the junction temperature of AlGaIn UV LEDs emitting at 295 nm is determined.<sup>2</sup> A  $2 \times 5$  array of  $0.3 \text{ mm} \times 0.3 \text{ mm}$  UV LEDs is mounted in a TO-257 package. The device contains three-finger-interdigitated  $p$  and  $n$  electrodes to improve the current spreading. The substrate-emitting LEDs<sup>2</sup> were grown by metalorganic vapor phase epitaxy on  $c$ -plane sapphire substrates using a  $2200 \text{ \AA}$  AlN buffer followed by a  $0.4\text{-}\mu\text{m}$ -thick undoped  $\text{Al}_{0.48}\text{Ga}_{0.52}\text{N}$  base layer. Next, a ten-period superlattice with  $100 \text{ \AA}$  AlN barriers and  $100 \text{ \AA}$   $\text{Al}_{0.60}\text{Ga}_{0.40}\text{N}$  wells was grown followed by a thick,  $0.85 \text{ }\mu\text{m}$  Si-doped,  $n$ -type  $\text{Al}_{0.48}\text{Ga}_{0.52}\text{N}$  current spreading layer.  $N$ -type  $\text{Al}_{0.48}\text{Ga}_{0.52}\text{N}$  current spreading layers have typical mobilities of  $\sim 55 \text{ cm}^2/\text{Vs}$  and carrier concentrations of  $\sim 2.5 \times 10^{18} \text{ cm}^{-3}$ . A multiple quantum-well active region was grown consisting of 3 periods of  $20 \text{ \AA}$   $\text{Al}_{0.36}\text{Ga}_{0.64}\text{N}$  wells and  $50 \text{ \AA}$  Si-doped  $\text{Al}_{0.48}\text{Ga}_{0.52}\text{N}$  barriers. The structure was completed with a  $100 \text{ \AA}$  Mg-doped  $\text{Al}_{0.60}\text{Ga}_{0.40}\text{N}$  layer, followed by a  $200 \text{ \AA}$   $p$ -GaIn contact layer.

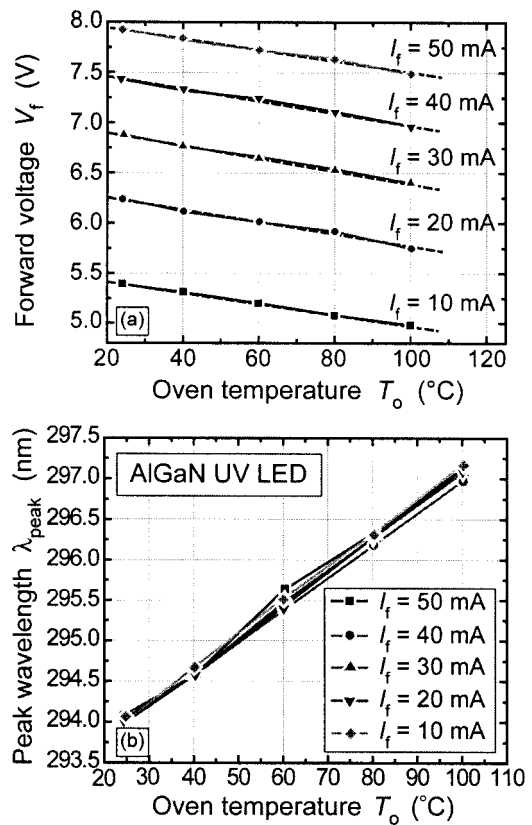


FIG. 2. (a) Experimental forward voltage and (b) peak position vs oven temperature for different pulsed injection currents. The dashed line is a linear fit to the experimental data.

Figure 1(a) shows the  $I$ - $V$  curve of the LED sample for pulsed and dc current. The forward voltage at 20 mA is 6.24 V. The reverse breakdown voltage of the diode is 13.1 V. The electroluminescence spectrum displays a narrow, clean line with full width at half maximum of 11.6 nm. The LED emission spectra for a forward current of  $I_f = 20 \text{ mA}$  under dc and pulsed condition are shown in Fig. 1(b). The peak emission wavelength is 294.6 nm. A low-intensity below-band-gap transition is found at the long-wavelength part of the electroluminescence spectrum. It has been shown<sup>2</sup> that the intensity of the below-band-gap transition decreases with increasing injection current, consistent with deep-level transitions.

During the calibration measurement, the pulsed current is increased from 10 to 50 mA in 10 mA increments. The measured forward-voltage-versus-oven-temperature relation is shown in Fig. 2(a). The dashed lines are linear fits to the experimental data. Figure 2(b) shows the measured peak-position-versus-oven-temperature calibration results. From Fig. 2(a), the experimental temperature coefficient is  $dV_f/dT = -5.8 \text{ mV/K}$ . For  $N_A = N_D = 10^{16} \text{ cm}^{-3}$ , the value calculated from Eq. (4) is  $-2.04 \text{ mV/K}$ , which is smaller than the experimental coefficient. The difference between the theoretical and experimental coefficients is attributed to a higher doping activation in the confinement regions at elevated temperatures. Higher doping activation increases the conductivity of the confinement regions thereby decreasing  $V_f$ .

Figure 3 shows the junction temperature versus the dc forward current by using diode forward voltage and emission peak shift. Both  $T_j$ -vs- $I_f$  curves shown in the figure are approximately linear. Linear fits of these curves are shown in

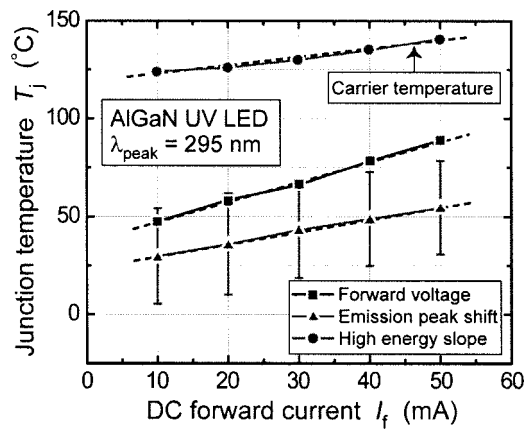


FIG. 3. Junction temperature as a function of dc forward current for an AlGaIn deep UV LED. Also shown is a linear fit for the experimental data (dashed line).

the same diagram. The junction temperature obtained by measuring diode forward voltage is most sensitive and its accuracy is estimated to be  $\pm 3$  °C. The junction temperature for  $I_f=20$  mA is 54 °C.

The junction temperature determined from the emission peak energy shift is less accurate than the forward-voltage method due to the spectral width of the emission spectra. It is commonly accepted that the accuracy of the peak energy value is about 10% of the emission linewidth. If the error bar caused by the uncertainty in peak position ( $\pm 24$  °C) and the error bar of the forward-voltage measurement ( $\pm 3$  °C) are taken into account, the first two methods are in good agreement, as shown in Fig. 3.

The temperature measured by using high energy slope method is the *carrier temperature*, which is higher than the lattice temperature at the junction. The high carrier temperature (from the top curve in Fig. 3) may be due to a high forward voltage and high-energy injection of carriers into the active region. The forward voltage increases from 5.2 to 7.7 V when the forward current increases from 10 to 50 mA, which is somewhat higher than the expected forward voltage. The broadening of the emission spectra due to unavoidable alloy composition fluctuations (alloy broadening) in the AlGaIn active region can increase the linewidth; decrease the high-energy slope, thereby increasing the apparent carrier temperature.

In order to reduce the thermal resistance of the sample, several experiments were conducted with different heat sinks. Three different curves are shown in Fig. 4 along with their thermal resistivities. The top curve corresponds to the packaged device, the middle curve corresponds to the device screwed on a large heat sink, and the bottom curve corresponds to the packaged device mounted with a good thermal contact on the heat sink. The thermal contact is established with a thermal paste from Commonwealth Scientific Corporation as used for microelectronics applications. The range of the junction temperature is between 43 and 87 °C when the dc forward current increases from 10 to 50 mA. The thermal resistance is as low as 87.6 K/W.

In conclusion, the junction and carrier temperatures for AlGaIn UV LEDs are measured using three methods. A linear relation between the junction temperature and the for-

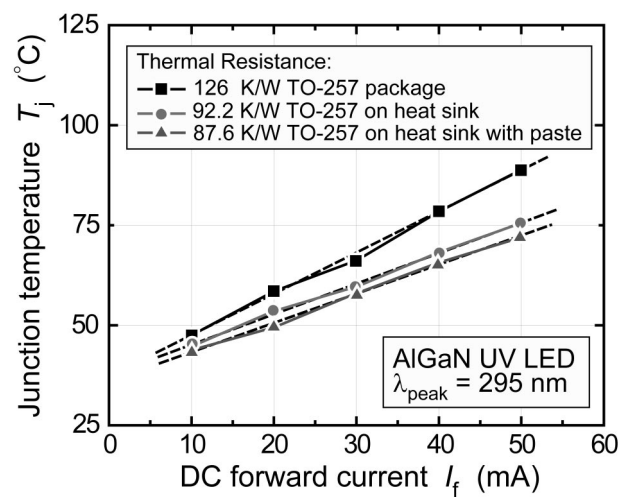


FIG. 4. Junction temperature as a function of dc forward current for an AlGaIn deep UV LED for different packaging conditions. Also shown is a linear fit for the experimental data (dashed line).

ward current is found. The experimental results indicate that diode forward-voltage method is the most accurate one ( $\pm 3$  °C) and can be used for a wide range of electronic and optoelectronic *pn*-junction devices. The junction temperature increases to 87 °C for the injection current of 50 mA. The difference in the theoretical and experimental temperature coefficient of forward voltage is attributed to the temperature coefficient of the confinement regions whose resistivity decreases with increasing temperature due to a higher doping activation. The thermal resistance of the sample mounted on a heat sink with thermal paste is 87.6 K/W.

Support at Rensselaer through the DARPA SUVOS program, ARO, and NSF is gratefully acknowledged. Sandia is a multiprogram laboratory operated by Sandia Corporation for the U. S. Department of Energy's National Nuclear Security Administration under Contract No. DE-AC04-94AL85000. Work at Sandia is supported by DARPA under the SUVOS program.

- <sup>1</sup>T. Mukai, D. Morita, and S. Nakamura, *J. Cryst. Growth* **778**, 189 (1998).
- <sup>2</sup>A. J. Fischer, A. A. Allerman, M. H. Crawford, K. H. A. Bogart, S. R. Lee, R. J. Kaplar, W. W. Chow, S. R. Kurtz, K. W. Fullmer, and J. J. Figiel, *Appl. Phys. Lett.* **84**, 3394 (2004).
- <sup>3</sup>D. Morita, M. Sano, M. Yamamoto, T. Murayama, S. Nagahama, and T. Mukai, *Jpn. J. Appl. Phys., Part 2* **41**, L1434 (2002).
- <sup>4</sup>S. Wu, V. Adivarahan, M. Shatalov, A. Chitnis, W. H. Sun, and M. Asif Khan, *Jpn. J. Appl. Phys., Part 2* **43**, L1035 (2004).
- <sup>5</sup>S. X. Jin, J. Li, J. Z. Li, J. Y. Lin, and H. X. Jiang, *Appl. Phys. Lett.* **76**, 631 (2000).
- <sup>6</sup>S. Todoroki, M. Sawai, and K. Aiki, *J. Appl. Phys.* **58**, 1124 (1985).
- <sup>7</sup>S. Murata and H. Nakada, *J. Appl. Phys.* **72**, 2514 (1992).
- <sup>8</sup>P. W. Epperlein, in *Proceedings of 17th International Symposium of Gallium Arsenide and Related Compounds*, IOP Conference Series Vol. 112 (IOP, London, 1990), p. 633.
- <sup>9</sup>P. W. Epperlein and G. L. Bona, *Appl. Phys. Lett.* **62**, 3074 (1993).
- <sup>10</sup>D. C. Hall, L. Goldberg, and D. Mehuys, *Appl. Phys. Lett.* **61**, 384 (1992).
- <sup>11</sup>Y. Gu and N. Narendran, *Proc. SPIE* **5187**, 107 (2004).
- <sup>12</sup>Y. Xi and E. F. Schubert, *Appl. Phys. Lett.* **85**, 2163 (2004).
- <sup>13</sup>J. Millman and C. Halkias, *Integrated Electronics* (McGraw-Hill, New York, 1972).
- <sup>14</sup>E. F. Schubert, *Light Emitting Diodes* (Cambridge University Press, Cambridge, UK, 2003).